Pak. J. Bot., 59(4): April 2027.

ARTICLE | DOI: http://dx.doi.org/10.30848/PJB2027-4(17)

SYNERGISTIC ANTI-INFLAMMATORY AND ANTIFUNGAL ACTIVITIES OF *ANVILLEA RADIATA* AND *COTULA CINEREA* ESSENTIAL OILS IN COMBINATION WITH CONVENTIONAL DRUGS AGAINST *ASPERGILLUS FUMIGATUS* AND *ASPERGILLUS TERREUS*

KHALDI ACHRAF[1,2]*, MAZERI AMINA[2] AND MEHDI KHEIRA[1,2]

[1]Laboratory of Valorization of Biological Resources and Food Security, University of Tahri Mohamed- Bechar, BP 417, 08000 Bechar, Algeria
[2]Department of Biology, Faculty of Sciences of Nature and Life, University of Tahri Mohamed- Bechar, BP 417, 08000 Bechar, Algeria

*Corresponding author's email: khaldi.achraf@univ-bechar.dz

Abstract

Essential oils (EOs) extracted from *Anvillea radiata* Coss. & Dur. and *Cotula cinerea* Del. were investigated for their chemical composition, anti-inflammatory, antifungal, and anti-gliotoxin activities, as well as their potential synergistic interactions with conventional drugs. Chemical profiles were determined using gas chromatography–mass spectrometry (GC–MS). Anti-inflammatory activity was evaluated by the bovine serum albumin denaturation assay, while antifungal activity was assessed through mycelial growth inhibition, minimum inhibitory concentration (MIC) determination, spore germination, and mycelial biomass assays. Anti-gliotoxin effects were also examined.

The main constituents of *A. radiata* EO were (Z)-nerolidol (64.53%), humulene epoxide II (10.59%), and epi-α-cadinol (7.45%), whereas *C. cinerea* EO was dominated by trans-thujone (17.32%), 1,8-cineole (13.96%), cis-verbenyl acetate (12.61%), camphor (11.74%), and santolina triene (10.80%). Both oils exhibited notable anti-inflammatory and antifungal activities against *Aspergillus fumigatus* and *A. terreus*. Synergistic interactions were observed when EOs were combined with the antifungal agent voriconazole or with each other, leading to reduced MIC values and enhanced inhibition of mycelial growth and spore germination. In contrast, anti-gliotoxin activity was more pronounced for individual EOs than for their mixtures. Overall, these results highlight the potential of *A. radiata* and *C. cinerea* EOs as promising natural agents with anti-inflammatory and antifungal properties, warranting further *in vivo* and toxicological studies to confirm their efficacy and safety.

Key words: Essential oil; Biological activities; Aspergillosis; Drug; Synergy

Introduction

Inflammatory diseases remain a major health concern worldwide, and their conventional management primarily relies on steroidal (SAIDs) and nonsteroidal anti-inflammatory drugs (NSAIDs). Despite their efficacy, these agents such as glucocorticoids, aspirin, ibuprofen, and indomethacin—are associated with numerous adverse effects, including gastrointestinal, cardiovascular, and renal complications, which limit their long-term use (Wang *et al.,* 2016). Consequently, there is an increasing demand for safer, plant-derived anti-inflammatory agents with comparable efficacy and fewer side effects.

Fungal infections, particularly those caused by species of the genus *Aspergillus*, also pose significant clinical challenges. This genus includes over 250 species of filamentous fungi that are opportunistic human pathogens and producers of mycotoxins and allergens. Among them, *Aspergillus fumigatus* and *A. terreus* are the principal causative agents of invasive aspergillosis (IA), a life-threatening disease in immunocompromised patients (Arabatzis *et al.,* 2013; Rudramurthy *et al.,* 2019; Ujie *et al.,* 2024). One of the key virulence factors associated with these species is gliotoxin, a secondary metabolite that impairs immune defense mechanisms and contributes to fungal pathogenicity (Kosalec & Pepeljnjak, 2005).

In recent years, medicinal plants and their essential oils (EOs) have attracted growing interest in pharmaceutical research due to their diverse pharmacological properties, including anti-inflammatory, antioxidant, and antifungal activities (Bliss *et al.,* 2022; Roana *et al.,* 2021). Furthermore, several studies have reported that combining EOs with conventional anti-inflammatory or antifungal drugs can yield synergistic effects, thereby reducing the required drug dosage and minimizing potential toxicity (Lima *et al.,* 2022; Mazeri *et al.,* 2024; Türk *et al.,* 2024). Such findings underscore the promising role of EOs as adjuvants in developing new therapeutic approaches for inflammation and fungal infections.

Plants belonging to the Asteraceae family are particularly renowned for their pharmacological potential, attributed to their high content of bioactive phytochemicals such as flavonoids, polyphenols, and terpenoids (Perveen *et al.,* 2020). *Anvillea radiata* Coss. & Dur. and *Cotula cinerea* Del. are two aromatic and medicinal species from this family, native to North Africa especially Algeria and Morocco where they are traditionally used for treating inflammation, infections, hypertension, diabetes, and wounds (Beniaich *et al.,* 2022; Mazeri *et al.,* 2024). Although numerous studies have investigated the biological properties of their individual EOs, research on

Received: 15-04-2026 | Revised: 18-09-2026 | Accepted: 27-09-2026 | Online: 05-11-2026

their combined effects remains scarce. Therefore, the present study aims to (i) characterize the chemical composition of *A. radiata* and *C. cinerea* essential oils, (ii) evaluate their anti-inflammatory, antifungal, and anti-gliotoxin activities, and (iii) assess their synergistic interactions both with each other and with conventional anti-inflammatory and antifungal drugs.

Materials and Methods

Plant material: The aerial parts of *A. radiata* and *C. cinerea* were collected in March 2024 from Beni Abbes (30° 07′ 54″ N, 2° 10′ 09″ W; 499 m a.s.l.) and Taghit (30° 55′ 03″ N, 2° 01′ 49″ W; 580 m a.s.l.) in Bechar Province, southwestern Algeria. The collection of plant materials was conducted in accordance with institutional and national guidelines and authorized by the Algerian Ministry of Higher Education and Scientific Research. Botanical identification was carried out by a qualified taxonomist, and voucher specimens (VUB112–VUB116) were deposited at the Laboratory of Valorization of Biological Resources and Food Security (VBRFS), Tahri Mohamed University of Bechar, Algeria. The plant materials were air-dried at room temperature prior to essential oil extraction.

Extraction and analysis of EOs: Dried plant materials were subjected to hydrodistillation for 4 hours using a Clevenger-type apparatus. The obtained EOs were dried over anhydrous sodium sulfate and stored in sealed amber vials at 4°C until analysis. The chemical composition of the EOs was determined by Gas Chromatography equipped with a Flame Ionization Detector (GC–FID; Hewlett-Packard HP 6890) and by Gas Chromatography coupled with Mass Spectrometry (GC–MS; Hewlett-Packard HP 6890/HP 5973), following the method described by (Khaldi *et al.,* 2017). The identification of constituents was achieved by comparing their mass spectra with those from the NIST 11 and Adams libraries, as well as by calculating retention indices relative to a homologous series of n-alkanes (C_8-C_{32}). The calculated indices were then compared with values reported in the literature for compound confirmation (Adams, 2017).

Anti-inflammatory activity: The anti-inflammatory activity of the EOs, individually and in combination (1:1, v/v), was evaluated using the Bovine Serum Albumin (BSA) denaturation assay, following the procedure described by (Mathouet *et al.,* 2020), with minor modifications. Stock solutions of each EO were prepared in 0.5% (v/v) dimethyl sulfoxide (DMSO). Solvent control samples containing the same concentration of DMSO but without EOs were included in all assays. Briefly, 450 µl of 0.5% BSA solution was mixed with 2.5 ml of phosphate-buffered saline (pH 6.3) and 50 µl of EO at different concentrations (0.1, 0.5, 1, 2.5, 5, and 10 mg/ml). Distilled water served as the negative control, while solvent controls (0.5% DMSO) were run in parallel. The mixtures were incubated at 55°C for 30 min, then cooled to room temperature. Absorbance was measured at 660 nm using a UV-visible spectrophotometer (Camspec M550). Diclofenac sodium was used as the reference anti-inflammatory drug. The inhibition of protein denaturation was calculated and expressed as a percentage. To evaluate the combined anti-inflammatory effects of EOs with each other and with diclofenac, isobologram analysis was performed based on the half-maximal inhibitory concentration (IC_{50}) values. Fractional inhibitory concentration at 50% (FIC_{50} I) indices were calculated as described by (Sharma *et al.,* 2020): FIC_{50} I = FIC_{50} (A) + FIC_{50} (B), where FIC_{50} (A) = IC_{50} (of A in the presence of B)/IC_{50} of A alone, and similarly for B. Combinations were classified as synergistic (FIC_{50} I < 0.9), additive (0.9 ≤ FIC_{50} I ≤ 1.1), or antagonistic (FIC_{50} I > 1.1). For each binary combination, the mean FIC_{50}I value was calculated from three concentration ratios. Isobolographic plots were constructed by plotting the IC_{50} values of combined treatments on axes representing the doses of each agent; concave-up curves located below the line of additivity (diagonal line) indicated synergy. All assays were performed in triplicate (technical replicates).

Antifungal activities

Fungal strains: The antifungal activity of the EOs was evaluated against two clinically isolated pathogenic fungal strains known to produce gliotoxin (GT): *Aspergillus fumigatus* and *Aspergillus terreus*. Both isolates were obtained from clinical specimens provided by the Laboratory of VBRFS, Tahri Mohamed University of Bechar, Algeria. The fungi were cultured on acidified Potato Dextrose Agar (PDA) and incubated in the dark at 27 ± 2°C for 7 days. Morphological identification of both strains was performed according to the taxonomic keys and diagnostic criteria described by (Pitt and Hocking, 2009), based on colony morphology, conidial structure, and vesicle characteristics. Molecular confirmation of the isolates was achieved by sequencing the ITS1–ITS4 region of rDNA, and the resulting sequences were compared with reference strains available in the NCBI GenBank database using BLAST analysis. Gliotoxin production was confirmed by Thin Layer Chromatography (TLC) as described by (Kosalec & Pepeljnjak, 2005), where bluish-green fluorescent spots under UV light (365 nm) indicated active toxin biosynthesis. Spore suspensions were prepared by gently scraping the colony surfaces and suspending the conidia in sterile 0.85% (w/v) sodium chloride solution containing 0.01% Tween 80 to facilitate dispersion. The spore concentration was adjusted to approximately 10^5 spores/ml using a Malassez hemocytometer to ensure standardized inoculum density for all assays.

Mycelial growth assay and assessing synergistic effect: The minimum inhibitory concentration for mycelial growth (MIC^m) of each EO and VOZ, was determined using the agar dilution method as described by (Khaldi *et al.,* 2017), with slight modifications. Stock solutions of each EO were prepared in 0.5% (v/v) DMSO and incorporated into PDA medium (15 ml/ petri plate). Twofold serial dilutions of EOs (210-15000 µg/ml) and VOZ (0.1110 µg/ml) were prepared, and 100 µl of each dilution was added to the PDA plates before solidification. Each plate was inoculated with 100 µl of a standardized spore suspension (10^5 spores/ml). Medium without EO or VOZ served as the growth control, whereas medium containing 0.5% DMSO without EO or

VOZ served as the solvent control. To determine the minimum fungicidal concentration (MIC^f), 5 mm mycelial plugs were excised from inhibited colonies, washed with sterile distilled water, and transferred onto fresh PDA plates. Fungal growth was observed after incubation at 27 ± 2°C for 7 days. Synergistic interactions between EOs and between EOs and VOZ (1:1 v/v) were evaluated using the checkerboard microdilution method as outlined by (Jiang *et al.,* 2023). Twofold serial dilutions of each treatment combination (*A. radiata* / *C. cinerea*, *A. radiata* / VOZ, and *C. cinerea* / VOZ) were prepared, ranging from 1/2 to 1/16 of the individual MIC values in 0.5% DMSO. In 96-well microtiter plates, 50 µl of EO (A) was dispensed horizontally across each row and 50 µl of EO (B) vertically down each column. Likewise, EO dilutions were combined with VOZ following the same scheme. From each well, 100 µl of the mixture was transferred onto PDA previously inoculated with 100 µl of the spore suspension. Plates were incubated at 27 ± 2 °C for 7 days. The Fractional Inhibitory Concentration Index (FICI) was calculated as: FICI=FIC of A + FIC of B; FIC of A = MIC of A in combination with B/MIC of A individually; FIC of B = MIC of B in combination with A/MIC of B individually. Where A and B are two different EOs/VOZ. Interactions were classified as synergistic (FICI ≤ 0.5), additive (0.5 < FICI ≤ 1), non-interactive (1 < FICI ≤ 4), or antagonistic (FICI > 4) following the criteria of (Nikkhah *et al.,* 2017). All assays were performed in triplicate (technical replicates).

Germination assay and measurement of FICI: The minimum inhibitory concentration for spore germination (MIC^g) of each EO and VOZ, was determined according to (Khaldi *et al.,* 2017), with minor modifications. Petri plates containing PDA supplemented with EOs or VOZ at the same concentrations used in the agar dilution method were prepared. A 100 µl aliquot of standardized spore suspension (10^5 spores/ml) was evenly spread over the surface of each plate. Plates containing PDA without EO or VOZ served as growth controls, while plates containing PDA with 0.5% (v/v) DMSO but without EO or VOZ served as solvent controls. All plates were incubated at 27 ± 2°C for 18 hours in the dark. The MIC^g was defined as the lowest concentration at which no visible germination occurred, as determined by microscopic counting of germinated versus ungerminated spores. Synergistic interactions between EOs and VOZ were further evaluated using the checkerboard microdilution assay (Jiang *et al.,* 2023). Serial twofold dilutions of each EO (A and B) and VOZ were prepared in 0.5% DMSO in 5 ml microtubes, then combined in 96-well microtiter plates to yield 1:1 (v/v) binary mixtures. Final concentrations ranged from 1/2 to 1/32 of the MIC. From each well, 100 µl of the resulting mixture was transferred onto PDA plates inoculated with 10 µl of the standardized spore suspension and evenly spread. Plates were incubated at 27 ± 2°C for 18 hours, and inhibition of germination was visually assessed. Growth control wells (without EO/VOZ or DMSO) and solvent controls were included in each plate. The Fractional Inhibitory Concentration Index (FICI) was calculated according to (Nikkhah *et al.,* 2017), following the procedure described in the previous section. All assays were performed in triplicate (technical replicates).

Anti-gliotoxin effect and assessing synergistic interaction: The biomass inhibition assay was performed according to (Khaldi *et al.,* 2017), with minor modifications to determine the minimum biomass inhibitory concentration (MIC^b). Stock solutions of each EO were prepared in 0.5% (v/v) DMSO and subsequently diluted in Yeast Extract Sucrose (YES) medium. Solvent control flasks containing the same concentration of DMSO without EOs or VOZ were included in all assays. In each 100 ml Erlenmeyer flask, 5 ml of the EO or VOZ dilution was added, and the total volume was adjusted to 50 ml with YES medium, yielding final concentrations of 210-6000 µg/ml for EOs and 0.1-8 µg/ml for VOZ. Control flasks contained no EO or VOZ. All flasks were inoculated with 100 µl of the standardized spore suspension and incubated at 27 ± 2 °C for 14 days. After incubation, the contents were filtered through pre-weighed filter papers, and the percentage inhibition of fungal biomass was calculated to determine MIC^b. For gliotoxin inhibition assessment, culture filtrates were extracted with chloroform and evaporated to dryness. The residues were dissolved in 1 ml of chloroform, and 50 µl aliquots were spotted on TLC plates (Silica Gel 60 G60, 0.25 mm). Chromatograms were developed using TEF solvent (toluene/ethyl acetate/formic acid, 50:40:10, v/v/v) and examined under UV light (365 nm). Developed plates were sprayed with 10% (w/v) aluminum chloride in 50% (v/v) ethanol and heated at 110°C for 10 minutes. Gliotoxin was identified by its characteristic bluish-green fluorescence and retention factor (Rf) matching that of the standard (Kosalec & Pepeljnjak, 2005). Synergistic interactions were evaluated by combining EOs (*A. radiata* / *C. cinerea*) or EOs with VOZ (1:1 v/v) using the checkerboard method described by (Das *et al.,* 2022). The Fractional Inhibitory Concentration Index (FICI) was calculated according to (Nikkhah *et al.,* 2017), following the same procedure outlined in the Mycelial growth assay and assessing synergistic effect section. All experiments were performed in triplicate using independent biological replicates.

Statistical analysis

All experiments were conducted in triplicate, including both biological and technical replicates. Statistical analyses were performed using one-way analysis of variance (ANOVA) with SPSS software (version 21.0). Significant differences among mean values were initially evaluated using Duncan's multiple range test at a 95% confidence level ($p<0.05$). To ensure more robust multiple comparisons and confirm consistency among treatment groups, Tukey's Honestly Significant Difference (HSD) test was also applied. All data are expressed as mean ± standard deviation (SD), and exact P-values are reported in the Results section to provide a precise indication of statistical significance. The interpretation thresholds for synergistic interactions varied depending on the experimental endpoint. For the anti-inflammatory assay, $FIC_{50}I$ values were interpreted according to (Sharma *et al.,* 2020), which provides appropriate synergy criteria for IC_{50}-based biochemical assays. In contrast, for antifungal, germination, and anti-gliotoxin assays, the FICI classification proposed by (Nikkhah *et al.,* 2017), was applied, as it is the standard reference for MIC-based antimicrobial tests. This distinction ensures methodological consistency and valid interpretation across different assay types.

Results

Essential oils composition: The extraction yield of *C. cinerea* EO was 0.90%, which is higher than the yield found for the EO of *A. radiata* of about 0.62%. The outcomes of the chemical analysis of the EOs are presented in Table 1. GC/MS analysis identified 20 and 46 compounds from *A. radiata* and *C. cinerea* EOs, respectively. From the specified components of the tested EOs in the two areas, 98.53% and 99.75% of the total EOs were identified, respectively. The *A. radiata* EO is predominately constituted of oxygenated sesquiterpenes, the main components were (Z)-nerolidol (64.53%), humulene epoxide II (10.59%), epi-α-cadinol (7.45%) and cis-chrysanthenyl acetate (4.04%), although oxygenated monoterpenes make up the majority of *C. cinerea*. EO, the major components were trans-thujone (17.32%), 1,8-cineole (13.96%), cis-verbenyl acetate (12.61%), camphor (11.74%), **s**antolina triene (10.80%) and ρ-Mentha-1,5-dien-8-ol (5.97%).

Anti-inflammatory activity: The findings from the assessment of anti-inflammatory properties using the BSA denaturation method are presented in Table 2. Among the tested EOs, *A. radiata* demonstrated superior efficacy in inhibiting thermal-induced protein denaturation, with an IC_{50} value of 2.72 ± 0.22 mg/ml ($P = 0.032$), compared to *C. cinerea* which exhibited an IC_{50} of 6.21 ± 0.32 mg/ml ($P = 0.028$). Both EOs showed significantly lower potency than the reference anti-inflammatory drug, diclofenac sodium (IC_{50} = 1.99 ± 0.13 mg/ml, $P = 0.034$). Regarding synergistic interactions, binary combinations of EOs and diclofenac exhibited synergistic effects, as reflected by $FIC_{50}I$ values of 0.85, 0.67, and 0.75, respectively. These combinations significantly enhanced anti-inflammatory activity compared to individual treatments ($P = 0.023$). The dose-response analysis further confirmed that EO-drug combinations were more effective across all tested concentrations. Moreover, the isobolographic analysis revealed concave-up isoboles, with all data points located below the line of additivity, confirming true synergistic interactions between the combined treatments (Fig. 1).

Each point represents the IC_{50} values of two agents in combination at different concentration ratios. The solid-colored lines indicate the experimental isobole, and the diagonal line connects the IC_{50} values of each compound tested alone represents the theoretical line of additivity ($FIC_{50}I = 1.0$). Points below the line indicate synergistic interactions ($FIC_{50}I < 0.9$), those on or near the line indicate additive effects ($0.9 \leq FIC_{50}I \leq 1.1$), and those above the line suggest antagonism ($FIC_{50}I > 1.1$). Each value represents the mean ± SD of three independent measurements (technical replicates).

Antifungal activities and anti-gliotoxin effect of single and combined application of essential oils. The antifungal activities and anti-gliotoxin effects of EOs and the antifungal reference drug, are summarized in Table 3. In all assays, fungal growth inhibition showed a significant correlation with MIC values ($P = 0.021$–0.039). Both EOs demonstrated inhibitory activity against fungal mycelial growth. *A. radiata* exhibited the strongest effect, with MIC^m values of 750 µg/ml for *A. fumigatus* and 1000 µg/ml for *A. terreus* ($P = 0.028$), whereas *C. cinerea* was comparatively less active, with MIC^m values of 3000 µg/ml and 11000 µg/ml, respectively ($P = 0.034$). By contrast, VOZ displayed markedly higher potency, with MIC^m values of 1 µg/ml and 2 µg/ml against *A. fumigatus* and *A. terreus* ($P = 0.022$). Similar trends were observed for the MIC^f, where *A. radiata* EO recorded values of 850 µg/ml (*A. fumigatus*) and 1100 µg/ml (*A. terreus*), compared to 3050 µg/ml and 11100 µg/m for *C. cinerea* EO ($P = 0.031$). VOZ exhibited MIC^f values of 2 µg/ml for both fungi ($P = 0.026$). Regarding spore germination inhibition, both EOs showed significant activity ($P = 0.024$). *A. radiata* EO displayed MIC^g values of 600 µg/ml (*A. fumigatus*) and 800 µg/ml (*A. terreus*), while *C. cinerea* EO required higher concentrations (2500 µg/ml and 10000 µg/ml, respectively). VOZ again proved most effective (0.5 µg/ml and 1 µg/ml, respectively). In the anti-gliotoxin assay, both oils demonstrated moderate activity, with inhibition of fungal biomass observed at MIC^b values of 1000 µg/ml (*A. fumigatus*) and 3000 µg/ml (*A. terreus*) for *A. radiata*, and 3200 µg/ml and 11200 µg/ml for *C. cinerea* EO ($P = 0.037$). VOZ exhibited MIC^b values of 4 µg/ml and 5 µg/ml against *A. fumigatus* and *A. terreus*, respectively ($P = 0.021$). The anti-gliotoxin test revealed no production of gliotoxin (absence of bluish-green fluorescence on TLC plates) for either fungal strain when treated at or above their respective MIC^b concentrations, confirming complete inhibition of toxin biosynthesis.

The synergistic and additive interactions between EOs and VOZ are detailed in Table 4. The combination of *A. radiata* (1/6 MIC) with *C. cinerea* (1/4 MIC) produced a synergistic effect against *A. fumigatus* (FICI = 0.41, $P = 0.025$), while the combination of *A. radiata* (1/4 MIC) with *C. cinerea* (1/2 MIC) exhibited an additive effect against *A. terreus* (FICI = 0.75, $P = 0.033$). Combinations of VOZ with each EO resulted in strong synergistic effects across all strains, with FICI values ranging from 0.31 to 0.49 ($P = 0.023$). Similarly, binary combinations targeting spore germination displayed consistent synergistic interactions, with FICI values ranging from 0.22 to 0.41 ($P = 0.019$). In biomass inhibition assays, EO–EO combinations showed no interactive effect against *A. fumigatus* (FICI = 2.5) and *A. terreus* (FICI = 3.25) ($P = 0.041$), whereas EO–VOZ combinations exhibited additive effects (FICI = 0.66–1.00) for most strains. Notably, the binary combination *A. radiata* (1/4 MIC) + VOZ (1/4 MIC) produced a synergistic interaction against *A. fumigatus* (FICI = 0.50, $P = 0.024$). Overall, out of 18 binary combinations tested, 12 (66.7%) demonstrated synergistic interactions (FICI ≤ 0.5), 4 (22.2%) showed additive effects (0.5 < FICI ≤ 1), and 2 (11.1%) exhibited no interactive effect (1 < FICI ≤ 4). No antagonistic interactions (FICI > 4) were detected in any of the assays. Interpretations of synergistic, additive, and non-interactive effects strictly followed the FICI classification criteria of (Nikkhah *et al.,* 2017), ensuring consistency between quantitative values and interaction terms across all experiments.

Table 1. Chemical composition of essential oils of *Anvillea radiata* Coss. & Dur. and *Cotula cinerea* Del. expressed in percentage (%).

Compounds	RT	RI	RI_{Lit}	Ss Aire [a]	Ss Aire [b]
2-methyl-1-butanol	02.49	727	724	-	0.14
(3Z)-Hexenol	04.08	852	850	-	0.20
2-Methyl butyl acetate	04.51	876	875	-	0.08
Santolina triene	05.14	908	906	-	**10.80**
tricyclene	05.56	924	921	-	0.16
α-thujene	05.67	929	924	-	1.70
α-pinene	05.89	936	932	2.12	2.35
camphene	06.30	950	946	0.22	2.70
Sabinene	06.91	972	969	-	3.26
β-pinene	07.08	978	974	0.15	0.74
myrcene	07.45	990	988	0.29	0.16
2,3,5-trimethyl-Pyrazine	07.78	1001	1000	-	0.05
iso-Sylvestrene	08.04	1008	1007	-	0.05
(2E,4E)-Heptadienol	08.29	1015	1013	-	0.04
α-terpinene	08.33	1017	1014	-	0.47
p-cymene	08.57	1024	1020	0.2	-
o-Cymene	08.65	1026	1022	-	1.11
limonene	08.73	1028	1024	0.3	-
1,8-Cineole	08.79	1029	1026	-	**13.96**
γ-Hexalactone	09.35	1044	1042	-	0.11
(3Z)-Octen-1-ol	09.53	1050	1047	-	0.25
γ-terpinene	09.83	1059	1054	-	1.08
5-hydroxy-4-Octanone	10.26	1069	1066	-	0.22
Dihydro myrcenol	10.37	1071	1069	-	0.40
terpinolene	11.00	1088	1086	-	0.20
linalool	11.34	1097	1095	0.1	0.37
Ipsenol	11.52	1103	1100	-	0.54
cis-Thujone	11.59	1104	1101	-	0.56
trans-Thujone	12.03	1115	1112	-	**17.32**
3-Octanol acetate	12.37	1122	1120	-	0.33
trans-Pinocarveol	13.02	1138	1135	0.09	0.33
camphor	13.30	1143	1141	-	**11.74**
ρ-Mentha-1,5-dien-8-ol	14.18	1165	1162	-	**5.97**
borneol	14.31	1167	1165	-	1.19
2-Methoxy-3-(1-methylpropyl) pyrazine	14.45	1171	1168	-	0.79
terpinen-4-ol	14.69	1177	1174	-	2.20
α-terpineol	15.24	1189	1186	-	1.85
Pulegone	17.29	1235	1233	-	0.58
cis-Chrysanthenyl acetate	18.54	1264	1261	**4.04**	-
cis-verbenyl acetate	19.37	1282	1280	-	**12.61**
Bornyl acetate	19.51	1286	1284	-	1.38
Lavandulyl acetate	19.72	1290	1288	-	0.57
thymol	19.74	1292	1289	-	0.12
(2E)-Hexenyl caproate	24.02	1388	1385	-	0.16
(Z)-Jasmone	24.30	1396	1392	-	0.20
α-Humulene	26.85	1455	1452	0.80	-
(E)-β-Farnesene	26.94	1456	1454	-	0.15
10,11-epoxy-Calamenene	28.49	1493	1491	-	0.22
α-Selinene	28.79	1503	1498	0.43	-
β-Bisabolene	29.07	1510	1505	0.65	-
(Z)-Nerolidol	30.13	1535	1531	**64.53**	-
α-Cadinene	30.36	1540	1537	3.6	-
Spathulenol	31.98	1579	1577	0.58	0.20
caryophyllene oxide	32.19	1585	1582	1.40	0.14
Humulene epoxide II	33.24	1612	1608	**10.59**	-
epi-α-Cadinol	34.42	1642	1638	**7.45**	-
epi-β-Bisabolol	35.64	1674	1670	0.45	-
α-Bisabolol	36.20	1688	1685	0.54	-
Total				98.53	99.75

RT: Retention time; RI: Retention index determined relative to a homologous series of n-alkanes (C_8-C_{32}) on the non-polar DB-5 capillary column; RI_{Lit}: Retention index literature (Adams, 2017); [a] *Anvillea radiata* Coss. & Dur.; [b] *Cotula cinerea* Del.

Table 2. Synergistic anti-inflammatory effect of essential oils and diclofenac sodium determined by the BSA denaturation method.

Treatment	IC_{50} (mg/ml)	IC_{50} * (mg/ml)	FIC_{50}	FIC_{50} I	FIC_{50} I average	Interaction
A. Combination*: Anvillea radiata* Coss. & Dur. */ Cotula cinerea* Del.						
A. radiata	2.72 ± 0.22 ^{c}	1.15 ± 0.28 $^{c, d}$	0.42	0.83	0.85	Synergistic
C. cinerea	6.21 ± 0.32 ^{b}	2.55 ± 0.15 $^{b,.d}$	0.41			
A. radiata	2.72 ± 0.22 ^{c}	1.35 ± 0.44 $^{c, e}$	0.49	0.85		
C. cinerea	6.21 ± 0.32 ^{b}	2.28 ± 0.12 $^{b e}$	0.36			
A. radiata	2.72 ± 0.22 ^{c}	1.45 ± 0.75 $^{c, f}$	0.53	0.87		
C. cinerea	6.21 ± 0.32 ^{b}	2.15 ± 0.19 $^{b, f}$	0.34			
B. Combination*: Anvillea radiata* Coss. & Dur. / Diclofenac						
A. radiata	2.72 ± 0.22 ^{a}	0.85 ± 0.03 $^{a d}$	0.31	0.82	0.67	Synergistic
diclofenac	1.99 ± 0.13 ^{b}	1.02 ± 0.10 $^{d, d}$	0.51			
A. radiata	2.72 ± 0.22 ^{a}	0.97 ± 0.08 $^{a, e}$	0.35	0.66		
diclofenac	1.99 ± 0.13 ^{b}	0.62 ± 0.09 $^{g, e}$	0.31			
A. radiata	2.72 ± 0.22 ^{a}	1.10 ± 0.07 $^{a, f}$	0.40	0.55		
C. Combination*: Cotula cinerea* Del. / Diclofenac						
C. cinerea	6.21 ± 0.32 ^{a}	2.10 ± 0.13 $^{i, d}$	0.33	0.88	0.75	Synergistic
diclofenac	1.99 ± 0.13 ^{c}	1.10 ± 0.25 $^{h, d}$	0.55			
C. cinerea	6.21 ± 0.32 ^{a}	2.35 ± 0.45 $^{i, e}$	0.35	0.75		
diclofenac	1.99 ± 0.13 ^{c}	0.80 ± 0.19 $^{h, e}$	0.40			
C. cinerea	6.21 ± 0.32 ^{a}	2.47 ± 0.42 $^{i, f}$	0.39	0.64		
diclofenac	1.99 ± 0.13 ^{c}	0.51 ± 0.11 $^{h, f}$	0.25			

IC_{50}*: IC_{50} values of combined treatments. Values represent mean ± standard deviation (n = 3). Distinct letters (a–i) indicate statistically significant differences among mean IC_{50} values according to one-way ANOVA followed by Duncan's multiple range test (P=0.021–0.048)
Note: Each combination was tested at three different concentration ratios. The corresponding IC_{50}*, FIC_{50}, and FIC_{50}I values were used to construct isobolographic plots. The FIC_{50}I average represents the mean of three calculated FIC_{50}I values per combination

Table 3. Antifungal activities and anti-gliotoxin effect [a] of tested essential oils against tested fungi

Fungal strain	Essential oils								Antifungal drug			
	Anvillea radiata Coss. & Dur.				*Cotula cinerea* Del.				VOZ			
	MIC^{m}	MIC^{f}	MIC^{g}	MIC^{b}	MIC^{m}	MIC^{f}	MIC^{g}	MIC^{b}	MIC^{m}	MIC^{f}	MIC^{g}	MIC^{b}
A. fumigatus	750	850	600	1000 ^{nf}	3000	3050	2500	3200 ^{nf}	1	2	0.5	4^{nf}
A. terreus	1000	1100	800	3000 ^{nf}	11000	11100	10000	11200 ^{nf}	2	2	1	5 ^{nf}

[a]: Results are expressed in µg/ml as mean ± standard deviation (n = 3). Statistical significance among treatments was determined using one-way ANOVA (P = 0.019–0.044). MIC^{m}: Minimum mycelial growth inhibitory concentration; MIC^{f}: Minimum fungicide concentration; MIC^{g}: Minimum germination inhibitory concentration; MIC^{b}: Minimum biomass inhibitory concentration; nf: Absence of fluorescence on TLC plate

Table 4. Synergistic effects of essential oils and Voriconazole against fungal strains

Fungal strain	Combination	MIC alone	MIC combination	FIC	FICI	Interaction
	Mycelial growth inhibition (MIC^{m})					
A. fumigatus	*A. radiata* + *C. cinerea*	750 / 3000	125 / 750	0.16 / 0.25	0.41	Synergistic
	A. radiata + VOZ	750 / 1	47 / 0.25	0.06 / 0.25	0.31	Synergistic
	C. cinerea + VOZ	3000 / 1	500 / 0.33	0.16 / 0.33	0.49	Synergistic
A. terreus	*A. radiata* + *C. cinerea*	1000 / 11000	250 / 5500	0.25 / 0.50	0.75	Additive
	A. radiata + VOZ	1000 / 2	83.3 / 0.66	0.08 / 0.33	0.41	Synergistic
	C. cinerea + VOZ	11000 / 2	1375 / 0.50	0.12 / 0.25	0.37	Synergistic
	Spore germination inhibition (MIC^{g})					
A. fumigatus	*A. radiata* + *C. cinerea*	600 / 2500	75 / 416.66	0.12 / 0.16	0.28	Synergistic
	A. radiata + VOZ	600 / 0.5	18.8 / 0.12	0.03 / 0.24	0.27	Synergistic
	C. cinerea + VOZ	2500 / 0.5	312.5 / 0.12	0.12 / 0.24	0.36	Synergistic
A. terreus	*A. radiata* + *C. cinerea*	800 / 10000	133.3 / 2500	0.16 / 0.25	0.41	Synergistic
	A. radiata + VOZ	800 / 1	50 / 0.16	0.06 / 0.16	0.22	Synergistic
	C. cinerea + VOZ	10000 / 1	2000 / 0.12	0.20 / 0.12	0.32	Synergistic
	Biomass inhibition and anti-gliotoxin effect (MIC^{b})					
A. fumigatus	*A. radiata* + *C. cinerea*	1000^{nf} / 3200^{nf}	500 / 6400	0.50 / 2	2.50	No interaction
	A. radiata + VOZ	1000^{nf} / 4^{nf}	250 / 1	0.25 / 0.25	0.50	Synergistic
	C. cinerea + VOZ	3200^{nf} / 4^{nf}	1600 / 1.33	0.50 / 0.33	0.83	Additive
A. terreus	*A. radiata* + *C. cinerea*	3000^{nf} / 11200^{nf}	6000 / 14000	2.00 / 1.25	3.25	No interaction
	A. radiata + VOZ	3000^{nf} / 5^{nf}	1000 / 1.66	0.33 / 0.33	0.66	Additive
	C. cinerea + VOZ	11200^{nf} / 5^{nf}	5600 / 2.5	0.50 / 0.50	1.00	Additive

nf: absence of fluorescence on TLC plate indicating inhibition of gliotoxin biosynthesis. MIC values given as µg/ml. Values represent mean ± standard deviation (n = 3). Statistical significance was assessed by one-way ANOVA followed by Tukey's HSD test (P = 0.012–0.049). FICI values were used to classify interaction types: synergistic (FICI ≤ 0.5), additive (0.5 < FICI ≤ 1), non-interactive (1 < FICI ≤ 4)

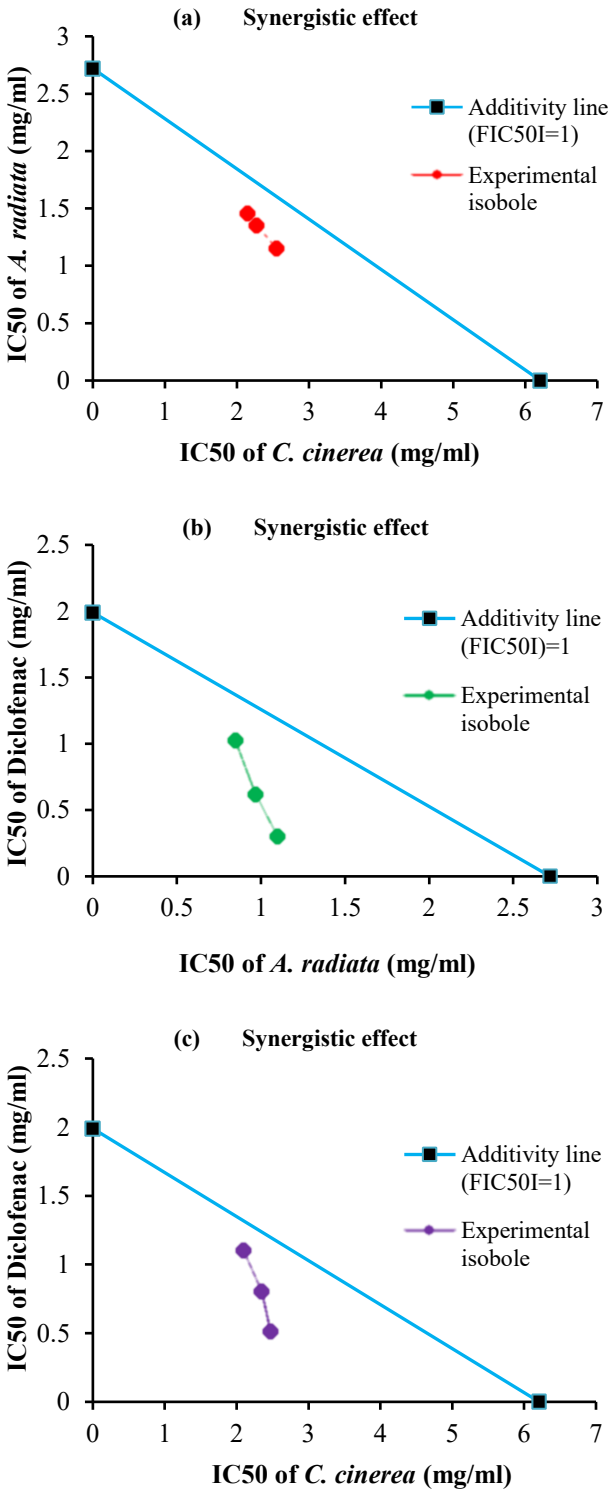


Fig. 1. sobolographic analysis of the anti-inflammatory interactions between *Anvillea radiata* Coss. & Dur., *Cotula cinerea* Del., and diclofenac sodium determined by the BSA denaturation assay. (a) *A. radiata* + *C. cinerea*; (b) *A. radiata* + Diclofenac; (c) *C. cinerea* + Diclofenac.

Discussion

Overall, the anti-inflammatory and antifungal activities of the essential oils (EOs) highlight their potential as natural therapeutic agents. However, their effectiveness may vary depending on the plant source, extraction method, and chemical composition (Bliss *et al.,* 2022; Roana *et al.,* 2021). In this study, among the identified constituents, epi-α-cadinol and cis-chrysanthenyl acetate have previously been reported as major components of *Anvillea garcinii* subsp. *radiata* EO (Oucheikh *et al.,* 2022a), whereas trans-thujone, 1,8-cineole, cis-verbenyl acetate, camphor, and santolina triene were predominant in *C. cinerea* EO (Boussoula *et al.,* 2016; Mazeri *et al.,* 2024). Other studies have described α-cuprenene, camphor, α-himachalene, 6-oxocyclonerolidol, and 6-hydroxycyclonerolidol as the principal constituents of *A. radiata* EO (El Hanbali *et al.,* 2007; Beniaich *et al.,* 2022), along with cis-8-acetoxychrysantenyl acetate and related sesquiterpenes in *A. garcinii* subsp. *radiata* (Oucheikh *et al.,* 2022a; Oucheikh *et al.,* 2022b). In the case of *C. cinerea*, 3-carene was identified as a major constituent (Chouikh *et al.,* 2015). These compositional variations likely reflect differences in geographical origin, environmental conditions, plant developmental stage, and harvesting time (Mutlu-Ingok *et al.,* 2020).

Protein denaturation is a widely recognized contributor to inflammation, and inhibition of this process is a common in vitro indicator of anti-inflammatory potential (Mathouet *et al.,* 2020). The anti-inflammatory activity observed for the tested EOs may be related to their major chemical constituents. In particular, the EO of *A. radiata* exhibited activity that could be mainly attributed to compounds such as (Z)-nerolidol, humulene epoxide II, and epi-α-cadinol. Nerolidol, a sesquiterpene alcohol commonly found in several medicinal plants, has been reported to inhibit the release of pro-inflammatory cytokines including TNF-α and IL-1β (Akhter *et al.,* 2022). Humulene epoxide II is recognized as a potential anti-inflammatory biomarker (Maiolini *et al.,* 2023), while epi-α-cadinol (T-cadinol) can reduce nitric oxide production in LPS-stimulated cells (González *et al.,* 2012). Similarly, the anti-inflammatory potential of *C. cinerea* EO may be primarily associated with 1,8-cineole (eucalyptol) and oxygenated monoterpenes such as trans-thujone and camphor, which have been reported to modulate the synthesis of inflammatory mediators (Bliss *et al.,* 2022; Stan *et al.,* 2019; Refaey *et al.,* 2022). Likewise, the reference anti-inflammatory drug diclofenac is known to inhibit prostaglandin synthesis and prevent the thermal denaturation of albumin (Ngoua-Meye-Misso. *et al.,* 2018). In agreement with our results, combinations of EOs with each other or with diclofenac produced enhanced inhibitory effects, suggesting possible synergistic interactions among their bioactive constituents. Although the BSA denaturation assay is a relatively basic and non-specific method, it remains a well-established preliminary screening tool for evaluating the anti-inflammatory potential of natural extracts and EOs due to its simplicity, reproducibility, and relevance to protein-stabilizing mechanisms. Nevertheless, this assay does not fully reflect the complexity of inflammatory responses in biological systems, and its limitations should be acknowledged. Future studies using cellular or animal inflammation models are therefore needed to confirm and expand upon the present findings (Ngoua-Meye-Misso *et al.,* 2018).

Previous studies have examined the antifungal activity of *A. radiata* Coss. & Dur. (syn. *A. garcinii* subsp. *radiata*) (Beniaich *et al.,* 2022; Oucheikh *et al.,* 2022a) and *C. cinerea* (Boussoula *et al.,* 2016; Dekinash *et al.,* 2017)

against diverse fungal species. In the present study, both EOs inhibited *A. fumigatus* and *A. terreus*, with a stronger effect on spore germination than on mycelial growth, suggesting preferential targeting of early developmental stages. Similar observations were made by (Moghtet *et al.,* 2017), who reported >80% inhibition of *A. fumigatus* growth by *A. radiata* extract, whereas (Dekinash *et al.,* 2017), found greater resistance to *C. cinerea* EO from Egypt. Regarding the reference antifungal drug, the MICs obtained for VOZ in our assays were higher than those defined by the Anon., 2020, which reports MIC values around 0.5 µg/ml for *A. fumigatus*. This discrepancy could be attributed to methodological and biological variations, such as differences in fungal strain sensitivity, inoculum size, medium composition, incubation time, or environmental factors affecting fungal physiology (Anon., 2020; Nikhil *et al.,* 2024). In addition, the use of EO matrices and mixed culture conditions may influence the apparent MIC values due to altered drug diffusion or potential interactions between volatiles and the azole compound (Mutlu-Ingok *et al.,* 2020). Nevertheless, our MIC for *A. fumigatus* was lower than that reported by (Nikhil *et al.,* 2024) (1.2 µg/ml), but higher for *A. terreus* than the value described by (Mohamadnia *et al.,* 2020), (0.25 µg/ml). These results highlight the variability in antifungal susceptibility among *Aspergillus* isolates and the importance of experimental standardization. The MICs obtained for spore germination inhibition (0.5-1 µg/ml) align well with those from earlier NCCLS reports (Espinel-Ingroff, 2001), supporting the overall reliability of our antifungal data.

Both *A. fumigatus* and *A. terreus* produce toxic secondary metabolites such as gliotoxin and terrein, which contribute to virulence by impairing host immunity (Kosalec & Pepeljnjak, 2005; Coméra *et al.,* 2007; Lass-Flörl *et al.,* 2021). Our findings showed that both EOs, particularly when combined with VOZ, inhibited gliotoxin-associated fluorescence, indicating suppression of toxin biosynthesis. The absence of bluish-green fluorescence on TLC plates may reflect inhibition of gliotoxin production or, alternatively, the formation of non-fluorescent complexes between EO constituents and gliotoxin intermediates (Khaldi *et al.,* 2017). While this hypothesis is speculative, it warrants further molecular validation through LC-MS or gene expression assays to clarify whether the inhibition results from direct chemical interactions or from suppression of the biosynthetic pathway. Although the TLC-based anti-gliotoxin assay is qualitative in nature, it was purposefully employed as a confirmatory screening method to determine whether the tested EOs could inhibit gliotoxin biosynthesis rather than to quantify the reduction of the toxin. The disappearance of fluorescence at MIC_b concentrations provides reliable preliminary evidence of inhibition. Nevertheless, future studies should complement this approach with quantitative methods such as HPLC to accurately assess the extent of gliotoxin suppression. Overall, the data support the antimycotoxigenic potential of *A. radiata* and *C. cinerea* EOs, consistent with prior reports of EOs disrupting fungal communication and mycotoxin synthesis (Lima *et al.,* 2022).

The antifungal effects of *A. radiata* EO are likely linked to its oxygenated sesquiterpenes, particularly sesquiterpene alcohols such as (Z)-nerolidol and epi-α-cadinol, which possess strong antifungal properties (Kacem *et al.,* 2016; Lara *et al.,* 2021). Similarly, the oxygenated monoterpenes in *C. cinerea* EO, notably eucalyptol, trans-thujone, and camphor, may contribute to its antifungal potential (Boussoula *et al.,* 2016; Dammak, 2019; Amine *et al.,* 2020). While the antifungal effects of individual EOs are known, this study is among the first to demonstrate their synergistic effects when combined. Mixtures of *A. radiata* and *C. cinerea* EOs showed enhanced inhibition of mycelial growth and spore germination compared to single oils, suggesting a true synergistic interaction. A similar enhancement was observed for EO/VOZ combinations. In contrast, EO/EO mixtures did not affect fungal biomass inhibition or gliotoxin suppression, confirming that synergy may depend on target processes (Jiang *et al.,* 2022). Such synergism likely arises from complementary actions of sesquiterpenes and monoterpenes, which can modify membrane permeability and facilitate antifungal drug uptake (Roana *et al.,* 2021; Hamdan *et al.,* 2024; Xie *et al.,* 2023). Conversely, non-interactive or antagonistic effects may occur when compounds share similar targets or interfere with each other's actions (Oliveira *et al.,* 2021). The contribution of minor constituents such as eucalyptol in combination with limonene, α-pinene, or p-cymene may also reinforce the overall synergistic effect (Sobhy *et al.,* 2023).

Mechanistically, EO-induced antifungal synergy may involve multiple pathways, including inhibition of ergosterol synthesis, disruption of cell wall and membrane integrity, interference with gene expression, and suppression of spore germination (Costa *et al.,* 2017; Jiang *et al.,* 2023). Plant-derived EOs are known to block ergosterol biosynthesis, an essential factor for fungal membrane stability (Saremi *et al.,* 2024). Similarly, VOZ targets cytochrome P450 dependent 14α-lanosterol demethylation (Nikhil *et al.,* 2024). The combined use of EOs and VOZ may therefore potentiate fungal inhibition by enhancing cell permeability, enabling greater drug uptake (Roana *et al.,* 2021). EO effects on spores may also involve enzyme denaturation or disruption of amino acid metabolism (Ben Miri *et al.,* 2023). Although these proposed mechanisms are consistent with the literature, they remain hypothetical and require further biochemical and molecular validation to elucidate the precise basis of the antifungal, anti-gliotoxin, and synergistic actions of these EOs.

Conclusion

The present study demonstrates that both Eos (*A. radiata* and *C. cinerea*) exhibit significant biological activities, including anti-inflammatory and antifungal effects against *Aspergillus* species responsible for aspergillosis. The observed synergistic interactions between these oils, and between the oils and conventional drugs, highlight their potential to enhance therapeutic efficacy when used in combination, particularly for mycelial growth inhibition and inflammation control. However, in the case of anti-gliotoxin activity, individual application of the oils proved more effective than combined use. These findings provide valuable insights into the possible synergistic mechanisms of EOs constituents and support their potential as complementary natural agents for managing fungal infections and

inflammation. Nevertheless, further *in vivo*, toxicological, and mechanistic studies are necessary to confirm their safety, bioavailability, and therapeutic applicability before any clinical use can be considered.

Acknowledgement

The authors would like to thank the pedagogical Biology laboratory of Tahri Mohamed Bechar University and the Directorate of post-graduation for their help and for providing all facilities to carry out this study.

Author's Contribution: Conceptualization, KA and MA; methodology, KA and MA; software, MA and MK; validation, KA and MK; formal analysis, KA and MA; investigation, KA, MA and MK; resources, KA and MA; data curation, KA and MA; writing—original draft preparation, KA; writing—review, editing, and paper communication, KA; visualization, KA and MK; supervision, KA and MK; All authors have read and agreed to the final version of the manuscript.

Conflict of Interest: The authors declare that there is no conflict of interest regarding the publication of this paper.

References

Adams, R.P. 2017. *Identification of Essential Oil Components by Gas Chromatography/Mass Spectrometry.* 4.1 ed., Texensis Publishing, USA. ISBN 978-1-932633-21-4.

Akhter, S., H.M. Irfan, Alamgeer, S. Jahan, M. Shahzad and M.B. Latif. 2022. Nerolidol: a potential approach in rheumatoid arthritis through reduction of TNF-α, IL-1β, IL-6, NF-kB, COX-2 and antioxidant effect in CFA-induced arthritic model. *Inflammopharmacol.*, 30: 537-548.

Amine, S., E.F. Kouoh, B. Eto, N. El Hamzaoui, A. Bouzoubaa, M. Mahjoubi and T. Zair. 2020. The antifungal effect of the main monoterpenes of the essential oil of *Artemisia herba-alba* var. *huguetii* (Caball.) Maire of the region of Ouarzazate-Morocco when tested against strains of *Candida*. *Res. J. Chem. Environ.*, 24(2): 111-117.

Anonymous. 2020. *Performance Standards for Antifungal Susceptibility Testing of Filamentous Fungi.* 2nd ed. CLSI supplement M61, Wayne, PA, USA.

Arabatzis, M. and A. Velegraki. 2013. Sexual reproduction in the opportunistic human pathogen *Aspergillus terreus*. *Mycologia*, 105(1): 71-79.

Ben Miri, Y., A. Benabdallah, A. Taoudiat, M. Mahdid, D. Djenane, Z. Tacer-Caba, C. Topkaya and J. Simal-Gandara. 2023. Potential of essential oils for protection of couscous against *Aspergillus flavus* and aflatoxin B1 contamination. *Food Control*, 145: 109474.

Beniaich, G., O. Hafsa, I. Maliki, Y.A. Bin Jardan, A. El Moussaoui, M. Chebaibi, A. Agour, O. Zouirech, H.A. Nafidi, F. Khallouki, M. Bourhia and M. Taleb. 2022. GC-MS characterization, in vitro antioxidant, antimicrobial and in silico NADPH oxidase inhibition studies of *Anvillea radiata* essential oils. *Horticulturae*, 8: 886.

Bliss, O., E. Emmanuel, N. Chigozie, E. Maureen and K. Michael. 2022. GC-MS characterization, in vitro antioxidant and anti-inflammatory activities of essential oil from the leaves of *Stachytarpheta jamaicensis*. *J. Mex. Chem. Soc.*, 66(4): 433-443.

Boussoula, E., M. Ghanmi, B. Satrani, M.B. Alaoui, R. Rhafouri, A. Farah, A. Nadine and C. Abdelaziz. 2016. Chemical quality, antibacterial and antifungal activities of *Cotula cinerea* essential oil from South Morocco. *Eurasian J. Anal. Chem.*, 12(5): 209-216.

Chouikh, A., B. Mayache, M.C. Maazi, Y. Hadef and A. Chefrour. 2015. Chemical composition and antimicrobial activity of essential oils in xerophytic plant *Cotula cinerea* Del. (Asteraceae) during two stages of development: flowering and fruiting. *J. Appl. Pharm. Sci.*, 5(3): 29-34.

Coméra, C., K. André, J. Laffitte, X. Collet, P. Galtier and I. Maridonneau-Parini. 2007. Gliotoxin from *Aspergillus fumigatus* affects phagocytosis and actin cytoskeleton organization in human neutrophils. *Microbes Infect.*, 9: 47-54.

Costa, M.D.C.M.F., A.G. Silva, A.P.S. Silva, V.L.M. Lima, P.C. Bezerra-Silva, S.K.L. Rocha, D.M.A.F. Navarro, M.T.S. Correia, T.H. Napoleão, M.V. Silva and P.M.G. Paiva. 2017. Essential oils from leaves of medicinal plants of Brazilian flora: Chemical composition and activity against *Candida* species. *Medicines.*, 4: 27.

Dammak, I., Z. Hamdi, S.K. El Euch, H. Zemni, A. Mliki, M. Hassouna and S. Lasram. 2019. Evaluation of antifungal and anti-ochratoxigenic activities of *Salvia officinalis*, *Lavandula dentata* and *Laurus nobilis* essential oils and a major monoterpene constituent 1,8-cineole against *Aspergillus carbonarius*. *Ind. Crops Prod.*, 128: 85-93.

Das, S., V.K. Singh, A.K. Chaudhari, Deepika, A.K. Dwivedy and N.K. Dubey. 2022. Co-encapsulation of *Pimpinella anisum* and *Coriandrum sativum* essential oils through binary mixture: antifungal mechanism and application as natural food preservative. *Pestic. Biochem. Physiol.*, 184: 105066.

Dekinash, M.F., T.N. Gryazneva, F.K. El-Fiky, H.A. Motawe, A.M. Beltagy and W.E. Soliman. 2017. Antimicrobial activity of the essential oil of *Cotula cinerea* against some pathogenic bacterial and fungal strains. *Vet. Sci. Anim. Sci. Biotechnol.*, 1: 86-91.

El Hanbali, F., A. El Hakmaoui, F. Mellouki, L. El Rhaffari and M. Akssira. 2007. Chemical composition and antibacterial activity of essential oil of *Anvillea radiata* Coss. & Dur. *Nat. Prod. Commun.*, 2(5): 595-597.

Espinel-Ingroff, A. 2001. Germinated and non-germinated conidial suspensions for testing susceptibilities of *Aspergillus* spp. to antifungal agents. *Antimicrob. Agents Chemother.*, 45(2): 605-607.

González, A.M., M.I. Tracanna, S.M. Amani, C. Schuff, M.J. Poch, H. Bach and C.A.N. Catalán. 2012. Chemical composition, antimicrobial and antioxidant properties of the volatile oil and methanol extract of *Xenophyllum poposum*. *Nat. Prod. Commun.*, 7(12): 1663-1666.

Hamdan, M., N. Jaradat, N. Al-Maharik, S. Ismail and M. Qadi. 2024. Chemical composition, cytotoxic effects and antimicrobial activity of combined essential oils from *Citrus meyeri*, *Citrus paradisi* and *Citrus sinensis* leaves. *Ind. Crops Prod.*, 210: 118096.

Jiang, H., S. Zhong, P. Schwarz, B. Chen and J. Rao. 2022. Chemical composition of essential oils from leaf and bud of clove and their impact on antifungal and mycotoxin inhibitory activities. *Ind. Crops Prod.*, 187: 115479.

Jiang, S., L. Wang, D. Li and C. Sun. 2023. Inhibitory effects of composite essential oils against dominant spoilage fungi on *Lonicera caeruleum*. *Food Biosci.*, 53: 102839.

Kacem, N., V. Roumy, N. Duhal, F. Merouane, C. Neut, P. Christen, K. Hostettmann and S. Rhouati. 2016. Chemical composition and antifungal activities of the essential oil from Algerian *Genista quadriflora* Munby. *Ind. Crops Prod.*, 90: 87-93.

Khaldi, A., B. Meddah, A. Moussaoui and P. Sonnet. 2017. Anti-mycotoxin effect and antifungal properties of essential oil from *Ammodaucus leucotrichus* Coss. & Dur. on *Aspergillus flavus* and *A. ochraceus*. *J. Essent. Oil Bear. Plants.*, 20: 36-44.

Kosalec, I. and S. Pepeljnjak. 2005. Mycotoxigenicity of clinical and environmental *Aspergillus fumigatus* and *A. flavus* isolates. *Acta Pharm.*, 55: 365-375.

Lara, L.L.S., V.A. Nascimento, C.C. Fernandes, M.R. Forim and C.M. Cazal. 2021. Chemical composition and antifungal activity of *Zanthoxylum riedelianum* stem bark essential oil. *Nat. Prod. Res.*, 36(6): 1653-1658.

Lass-Flörl, C., A.M. Dietl, D.P. Kontoyiannis and M. Brock. 2021. *Aspergillus terreus* species complex. *Clin. Microbiol. Rev.*, 34: e00311-20.

Lima, B., M. Sortino, A. Tapia and G.E. Feresin. 2022. Synergistic antifungal effectiveness of essential oils from Andean plants combined with commercial drugs. *Int. J. Pharm. Sci. Dev. Res.*, 8(1): 23-31.

Maiolini, T.C.S., K.J. Nicácio, W. Rosa, D.O. Miranda, M.F.C. Santos, P.C.P. Bueno and M.G. Soares. 2023. Potential anti-inflammatory biomarkers from Myrtaceae essential oils revealed by untargeted metabolomics. *Nat. Prod. Res.*, 39(4): 985-992.

Mathouet, H., C.S. Obiang, J.M. Abogo, H.P. Bourobou Bourobou and J.P. Ondo. 2020. Study of anti-inflammatory activity in vitro of four essential oils from Gabon. *Sch. Acad. J. Pharm.*, 9(1): 1-4.

Mazeri, A., A. Khaldi and K. Mehdi. 2024. Antibacterial and antioxidant activities of *Saccocalyx satureioides* Coss. & Dur. and *Cotula cinerea* Del. essential oils and their synergistic interactions. *Fresenius Environ. Bull.*, 33(4): 284-295.

Moghtet, S., N. Menad, B. Meddah and A. Moussaoui. 2017. *Anvillea radiata* (aerial parts): antifungal effect on mycotoxigenic fungi. *Int. J. Pharm. Sci. Rev. Res.*, 43(1): 32-34.

Mohamadnia, A., Z. Salehi, Z. Namvar, P. Tabarsi, M. Pourabdollah-Toutkaboni, S. Rezaie, M. Marjani, A. Moniri, Z. Abtahian, S.A. Mahdaviani, V. Mortezaee, E. Askari and S. Sharifynia. 2020. Molecular identification, phylogenetic analysis and antifungal susceptibility patterns of *Aspergillus nidulans* and *A. terreus* complexes isolated from clinical specimens. *J. Mycol. Med.*, 30(3): 101004.

Mutlu-Ingok, A., D. Devecioglu, D.N. Dikmetas, F. Karbancioglu-Guler and E. Capanoglu. 2020. Antibacterial, antifungal, antimycotoxigenic and antioxidant activities of essential oils: an updated review. *Molecules.*, 25: 4711.

Ngoua-Meye-Misso, R.L., S.O. Cédric, N.J.D.L. Croix, O.J. Privat, O.A. Felix and O.N. Louis-Clément. 2018. Phytochemical screening, antioxidant, anti-inflammatory and antiangiogenic activities of *Lophira procera* A. Chev. (*Ochnaceae*) medicinal plant from Gabon. *Egypt. J. Basic Appl. Sci.*, 5: 80-86.

Nikhil, A., A.K. Tiwari, R. Tilak, S. Kumar, P.S. Bharti, P.C. Pandey, R.J. Narayan and M.K. Gupta. 2024. Vancomycin-conjugated polyethyleneimine-stabilized gold nanoparticles attenuate germination and show potent antifungal activity against *Aspergillus* spp. *Appl. Sci.*, 14: 6926.

Nikkhah, M., M. Hashemi, M.B. Habibi Najafi and R. Farhoosh. 2017. Synergistic effects of some essential oils against fungal spoilage on pear fruit. *Int. J. Food Microbiol.*, 257: 285-294.

Oliveira Filho, J.G., G.C. Silva, H.M.C. Azeredo and M.D. Ferreira. 2021. Antifungal activity of essential oils and their combinations against postharvest fruit pathogens. *Acta Hortic.*, 1325: 183-190.

Oucheikh, L., O. Ou-Ani, S. Moujane, A. Ansari, A. Oubair and M. Znini. 2022a. Chemical composition, in vitro antifungal activity, DFT, molecular docking and molecular dynamics simulation studies of the essential oil from *Anvillea garcinii* subsp. *radiata* (Coss. & Durieu) Anderb. *J. Essent. Oil Res.*, 35(1): 35-50.

Oucheikh, L., O. Ou-Ani, Y. Youssefi, A. Oubair, M. Znini, J. Costa and L. Majidi. 2022b. Chemical diversity of essential oils from different organs of the Moroccan endemic medicinal plant *Anvillea garcinii* subsp. *radiata*. *J. Essent. Oil Bear. Plants.*, 25(1): 20-27.

Perveen, S., J. Alqahtani, R. Orfali, H.Y. Aati, A.M. Al-Taweel, T.A. Ibrahim, A. Khan, H.S. Yusufoglu, M.S. Abdel-Kader and O. Taglialatela-Scafati. 2020. Antibacterial and antifungal sesquiterpenoids from aerial parts of *Anvillea garcinia*. *Molecules.*, 25: 1730.

Pitt, J.I. and A.D. Hocking. 2009. *Fungi and Food Spoilage*. 3rd ed. Springer, Dordrecht, Heidelberg, London, New York, Cambridge, 519 pp.

Refaey, M.S., M.E. Abouelela, E.A.M. El-Shoura, H.M. Alkhalidi, S.A. Fadil, S.S. Elhady and R.F.A. Abdelhameed. 2022. In vitro anti-inflammatory activity of *Cotula anthemoides* essential oil and in silico molecular docking of its bioactives. *Molecules.*, 27: 1994.

Roana, J., N. Mandras, D. Scalas, P. Campagna and V. Tullio. 2021. Antifungal activity of *Melaleuca alternifolia* essential oil and its synergy with itraconazole or ketoconazole against *Trichophyton rubrum*. *Molecules*, 26(2): 461.

Rudramurthy, S.M., R.A. Paul, A. Chakrabarti, J.W. Mouton and J.F. Meis. 2019. Invasive aspergillosis by *Aspergillus flavus*: epidemiology, diagnosis, antifungal resistance, and management. *J. Fungi (Basel).*, 5(3): 55.

Saremi, G., M. Shams-Ghahfarokhi, A. Eslamifar, F. Jamzivar and M. Razzaghi-Abyaneh. 2024. Antifungal activity, synergistic effect and mode of action of caraway (*Carum carvi* L.) essential oil and carvone against *Aspergillus fumigatus*. *S. Afr. J. Bot.*, 168: 588-594.

Sharma, K., S. Guleria, V.K. Razdan and V. Babu. 2020. Synergistic antioxidant and antimicrobial activities of essential oils of selected medicinal plants in combination and with synthetic compounds. *Ind. Crops Prod.*, 154: 112569.

Sobhy, M., S.S. Ali, H. Cui, L. Lin and S. El-Sapagh. 2023. Exploring the potential of 1,8-cineole from cardamom oil against food-borne pathogens: antibacterial mechanisms and its application in meat preservation. *Microb. Pathog.*, 184: 106375.

Stan, M.S., S.N. Voicu, S. Caruntu, I.C. Nica, N.K. Olah, R. Burtescu, C. Balta, M. Rosu, H. Herman, A. Hermenean and A. Dinischiotu. 2019. Antioxidant and anti-inflammatory properties of *Thuja occidentalis* mother tincture for the treatment of ulcerative colitis. *Antioxidants (Basel).*, 8(9): 416.

Türk, S., Ş.G. Aşçı, T. Sevimoglu and S. Döşler. 2024. Investigating the antifungal, antioxidant and antibacterial activities of *Ocimum basilicum* L. and *Mentha piperita* L. essential oils and their synergistic potentials with antibiotics. *Istanbul J. Pharm.*, 54(1): 49-60.

Ujie, Y., S. Saito, K. Fukaya, D. Urabe, T. Yaguchi and A.A. Midori. 2024. *Aspergillus terreus* IFM 65899–THP-1 cell interaction triggers production of butyrolactone Ia, an immune suppressive compound. *Sci. Rep.*, 14: 28278.

Wang, Y.T., L. Zhu, D. Zeng, W. Long and S.M. Zhu. 2016. Chemical composition and anti-inflammatory activities of essential oil from *Trachydium roylei*. *J. Food Drug Anal.*, 24(3): 602-609.

Xie, Y., Y. Cao, T. Zhang, F. Liu, H. Liu and X. Xiao. 2023. Synergistic antifungal properties of lauraldehyde and geraniol against *Aspergillus flavus* in pistachio. *Food Control*, 153: 109915.